Heat Transfer Effect of Inert Gas on Multi-Tubular Reactor for Partial Oxidation Reaction

Kwang Ho Song[†], Sang Eon Han and Kwang-Ho Park

LG Chem Research Park, LG Chemical Ltd., Yu-song P.O. Box 61, Taejon 305-380, Korea

Abstract—The heat transfer effect of an inert gas on a multi-tubular reactor for a partial oxidation reaction has been determined. The model reaction system in the study was partial oxidation of propylene to acrolein. Both theoretical modeling and experimental studies have been performed to determine the heat transfer effect of inert gas on the system. Among many inert gases, CO_2 was selected and tested as a diluent gas for the partial oxidation of propylene to acrolein system instead of conventionally used N_2. The productivity increase through changing the inert gas from N_2 to CO_2 was possible due to the heat transfer capability of CO_2. In this study, by replacing the inert gas from N_2 to CO_2, productivity increased up to 14%.

Key words: Multi-tubular Reactor, Inert Gas, Heat Transfer, Acrolein, Carbon Dioxide

INTRODUCTION

Multi-tubular reactors are designed for reactions that generate a large amount of heat [Satterfield, 1970]. Due to the unique characteristic of easy heat removal, multi-tubular reactors are widely used for partial oxidation reaction processes. A multi-tubular reactor usually has more than 10,000 reaction tubes. The heat transfer medium, which is made of molten salt, circulates between the reaction tubes and removes heat from them. Heat transfer of reaction heat from the reactor tubes to the heat transfer medium is crucial for partial oxidation reaction processes. Detailed descriptions of multi-tubular reactors can be found elsewhere [Franzen et al., 1964; Jung et al., 1999].

Since the reactant is a flammable gas and has a possibility of explosion, a large amount of inert gas is fed into the reactor along with reactants. Inert gas also plays a role of heat transfer agent because it takes up a large portion of reactant gas mixture. Among many partial oxidation reactions, partial oxidation of propylene to acrolein was selected as a model system to investigate the heat transfer effect of inert gases. Usually N_2 is used as a diluent gas in the case of propylene partial oxidation to acrolein. N_2 gas consists of more than 50% of total input gas by volume in propylene partial oxidation to acrolein.

Different inert gases can be applied to this reaction system as a diluent gas. When an inert gas is mixed with reactants, there exists a specific ratio of mixture that becomes flammable or explosive. This specific ratio of mixture also depends on temperature and pressure of the reaction system. Usually, this ratio of mixture has a lower and upper boundary at constant temperature and pressure. If the range of this boundary for another inert gas is narrower than that of N_2, that inert gas is considered to be a better diluent gas in terms of safety. The productivity can also be increased while using the inert gas that has a narrower flammability or explosion range because more reactants can be fed into the multi-tubular reactor. Although

a selected inert gas may meet the flammability limitation, the heat transfer ability of the gas is also very important for partial oxidation reactions. If the reaction heat is not removed properly, the temperature will rise above normal operating conditions, possibly resulting in a run-away situation inside the reactor. When this happens to the reactor, there will be severe damage to the catalyst.

In an effort to find a better diluent gas for this model system of propylene partial oxidation to acrolein, CO_2 has been applied to the reaction system instead of N_2 gas and compared with the standard case of N_2. CO_2 has a narrower flammability or explosion range than N_2 for the present combination of inlet mixture gases [Song and Park, 1998]. Since CO_2 is better than N_2 in terms of the flammability limitation, only the heat transfer effect of inert gases will be considered in this study. Both experimental and theoretical studies have been performed to analyze the effect of inert gas on partial oxidation of propylene to acrolein.

EXPERIMENTAL

The schematic diagram of the experimental apparatus is shown in Fig. 1. The reactor used in the experiment is a jacketed single tubular reactor [Choi and Eigenberger, 1989]. Since it is very dif-
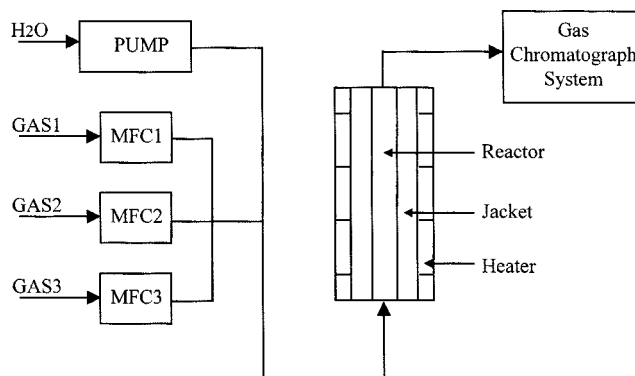

Fig. 1. The schematic diagram of the experimental apparatus.

[†]To whom correspondence should be addressed.
E-mail: khsong@lgchem.co.kr

ficult to make a lab-scale multi-tubular reactor, a single tubular reactor that exhibits the same characteristics of a multi-tubular reactor was made instead. The reactor consists of a 2.54 cm outer diameter stainless steel tube and an outer jacket made of 7.62 cm outer diameter stainless steel pipe. The wall thickness of the reactor tube was 1.651 mm. The heater was placed outside of the jacket. The length and diameter of the heater were 90 cm and 30 cm, respectively. The reactants and inert gas are fed into the reactor by using a Brooks mass flow controller. Water was pumped into the heated stainless steel tube by using a Hitachi L-7110 constant mass syringe pump. Water was then evaporated into steam and mixed with both reactants and inert gas. The molten salt, a mixture of $NaNO_2$, $NaNO_3$, and KNO_3, was used as the heat transfer medium, which supplies and removes heat from the fixed bed reactor. A thermowell tube of 0.398 cm outer diameter was mounted coaxially at the center of the reactor tube and also inside of the jacket, respectively. A mobile thermocouple was placed inside of the thermowell tube located at the center of the reactor so that the temperature could be measured along the length of the reactor. Additionally, three fixed thermocouples were placed inside of the jacket pipe in order to measure the temperature of the heat transfer medium at three different locations. The products were analyzed by a Hewlett-Packard gas chromatograph HP6800. Gas chromatography provided on-line analysis of a sample through a computer. Two different types of columns were used simultaneously to analyze the product gas: an Altech AT-1000 capillary column and a Hewlett-Packard chromosorb 102 packed column. Two different sizes of cylindrical shape catalysts were used for the experiments. A detailed description of the catalyst used in this investigation can be found elsewhere [Byun and Lee, 1999; Ko et al., 1998]. Alumina, as an inert material, large and small size catalysts were charged into the reactor in series. The heights of the Alumina and catalyst beds were 5.2 cm, 10.9 cm, and 30.4 cm, respectively. The amount of catalysts charged in the reactor was 32 g for the large size catalyst and 91 g for the small size catalyst.

The solid mixture of $NaNO_2$, $NaNO_3$, and KNO_3, was the heat transfer medium. It was melted by using the heater placed outside of the jacket. After temperature of the heat transfer medium reached the pre-set value, the reactants were fed into the reactor. It took at least 72 hours to reach the steady state. The experimental conditions are shown in Table 1.

MODELING

Since partial oxidation of propylene is a highly exothermic reaction, there remains the possibility that the temperature of the fluid phase may be much different from that of the solid phase. This leads to the necessity for introducing a heterogeneous model. The consideration of intraparticle gradients in the heterogeneous model is ap-

propriate for the present reaction system because it is important to predict precisely the maximum temperature of the solid phase. In general, the radial gradients can be neglected for all practical purposes if the radial aspect ratio $m(=R/d_p)$ does not exceed 4 [Carberry, 1976]. In the present experiment, the value of m was 2.7 and 3.2 for the two different sizes of catalyst beds, respectively. All of these values justify the usage of a one-dimensional heterogeneous model accounting for intraparticle gradients. The reaction kinetic model and parameters of Tan et al. [Tan et al., 1989] were adopted in this investigation. The model equation was derived from steady state mass and energy balances for fluid and solid phases as follows [Froment and Bischoff, 1979]:

Fluid Phase:

$$-\frac{d(u_s C_i)}{dz} + \varepsilon D_{ea} \frac{d^2 C_i}{dz^2} = k_{gi} a_v (C_i - C_{is}^s) \tag{1}$$

$$\frac{d(\rho_g u_s c_p T/M_w)}{dz} - \lambda_{ea} \frac{d^2 T}{dz^2} = h_f a_v (T_s^s - T) - 4\frac{U}{d_t}(T - T_r) \tag{2}$$

Solid Phase:

$$\frac{1}{r}\frac{d}{dr}\left(D_{ei} r \frac{dC_{is}}{dr}\right) - \rho_s r_i = 0 \tag{3}$$

$$\frac{1}{r}\frac{d}{dr}\left(\lambda_e r \frac{dT_s}{dr}\right) + \rho_s [(-\Delta H_1)k_1 + (-\Delta H_2)k_2 + (-\Delta H_3)k_3]C_4 \theta_x = 0 \tag{4}$$

where i=1, 2, 3, …, 7.
1: acrolein; 2: CO_2; 3: acetaldehyde; 4: propylene; 5: H_2O; 6: O_2; 7: N_2
The rate coefficients k_i(i=1, 2, 3) in Eq. (4) correspond to k_{12}, k_{13}, k_{14} of Tan et al. [Tan et al., 1989].

Boundary conditions
Fluid Phase:

$$u_s(C_{i0} - C_i) = -\varepsilon D_{ea} \frac{dC_i}{dz} \qquad \text{at z=0} \tag{5}$$

$$\frac{u_s \rho_g c_p}{M_w}(T_0 - T) = -\lambda_{ea} \frac{dT}{dz} \qquad \text{at z=0} \tag{6}$$

$$\frac{dC_i}{dz} = \frac{dT}{dz} = 0 \qquad \text{at z=L} \tag{7}$$

Solid Phase:

$$\frac{dC_{is}}{dr} = \frac{dT_s}{dr} = 0 \qquad \text{at r=0} \tag{8}$$

$$-D_{ei}\frac{dC_{is}}{dr} = k_{gi}(C_{is}^s - C_i) \qquad \text{at r=R} \tag{9}$$

Table 1. Experimental conditions

Run	Inert gas	C_3H_6 flow rate (m³/min)	O_2 flow rate (m³/min)	H_2O flow rate (m³/min)	Total flow rate (m³/min)	Inlet temp. (K)	Jacket temp. (K)	Reactor pressure (atm)
1	N_2	0.014	0.026	0.015	0.2	423	581	1
2	CO_2	0.014	0.026	0.015	0.2	423	581	1
3	CO_2	0.016	0.030	0.015	0.2	423	581	1

$$-\lambda_e \frac{dT_s}{dr} = h_f(T_s^s - T) \qquad \text{at } r=R \qquad (10)$$

Since density changes in the axial direction, the velocity also changes to satisfy the continuity equation:

$$u_s \rho_g = \text{constant} \qquad (11)$$

Many correlations for mass and heat transport are available in the literature, but there are strong deviations among them especially for heat transport. The temperature profile was shown from the numerical experiment to be dependent more upon the heat transfer coefficient than the mass transfer coefficient. Because of the lack of sufficient certainty in mass and heat transfer coefficients, it seemed reasonable to use a correlation which best fit the experimental data even though the catalyst used in the present experiment was different from that used in the work of Tan et al. [Tan et al., 1989]. The Petrovic and Thodos [Petrovic and Thodos, 1968] correlation for mass transport and the Rowe et al. [Rowe et al., 1965] correlation for heat transport were put to use in the modeling. The wall heat transfer coefficient was found to have much more effect on the temperature profile than the heat transfer coefficient between the fluid and the solid phase in the modeling. Many empirical correlations such as Leva and Grummer, Hanratty, Yagi and Kunii, De Wasch and Froment [Doraiswamy and Sharma, 1984], Calderbank and Pogorski [Calderbank and Pogorski, 1957], and Beek [Szekely et al., 1976] were tested. The equation of Calderbank and Pogorski [Calderbank and Pogorski, 1957] among many empirical correlations was found to fit best to the present experimental results.

The model equations were solved by using finite difference methods with an upwind scheme [Roach, 1972]. Since large sets of coupled nonlinear equations are difficult to converge unless an appropriate initial guess is given, equivalent unsteady state equations were constructed and made to march until the steady state was reached. It was sufficient to apply the pseudo-transient scheme only to the fluid phase equations. Since the transient solution was not of interest, the time steps were chosen to minimize computation time. The nonlinear equations were effectively solved with the successive over relaxation method.
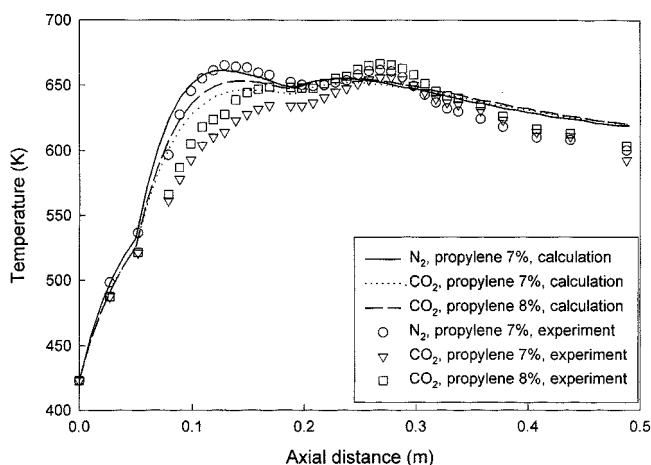
RESULTS AND DISCUSSION

Fig. 2. Experimental and calculated axial temperature profiles of the fluid phase in the case of N_2 and CO_2.

The experimental conditions are described in Table 1. The first experimental condition shown in Table 1 is a standard operating condition of propylene partial oxidation to acrolein. All the results obtained from using CO_2 as a diluent gas are compared with this standard case. The experimental and calculated temperature profiles of the fluid phase are compared in Fig. 2 for both diluent gases N_2 and CO_2, where similar shapes are observed. The discrepancies between the experimental and modeling results may be mainly attributed to the difference in reaction kinetics and the poor validity of the wall heat transfer correlation equation. In both cases of modeling and experimental results, the fluid phase temperature profile was lowered by the adoption of CO_2 as a diluent gas instead of N_2.

The modeling results of propylene concentration and temperature profiles of the solid phase, in the case of N_2 as a diluent gas, are given in Figs. 3 and 4, respectively. The concentration of propylene decreases with axial distance as the reaction proceeds. The
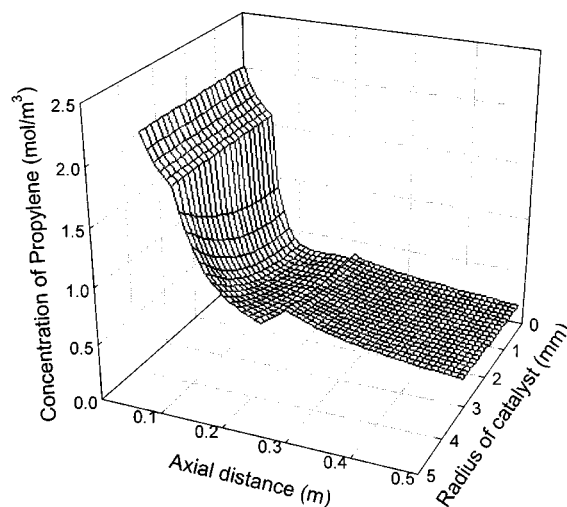

Fig. 3. Three-dimensional calculated propylene concentration profile of the solid phase in the case of experimental condition 1 shown in Table 1.
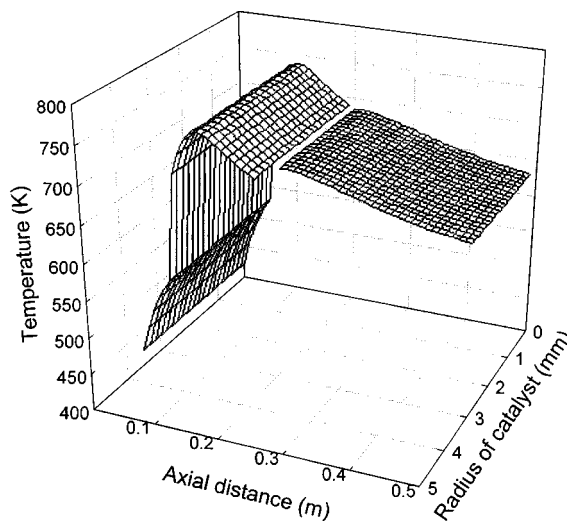

Fig. 4. Three-dimensional calculated temperature profile of the solid phase in the case of experimental condition 1 shown in Table 1.
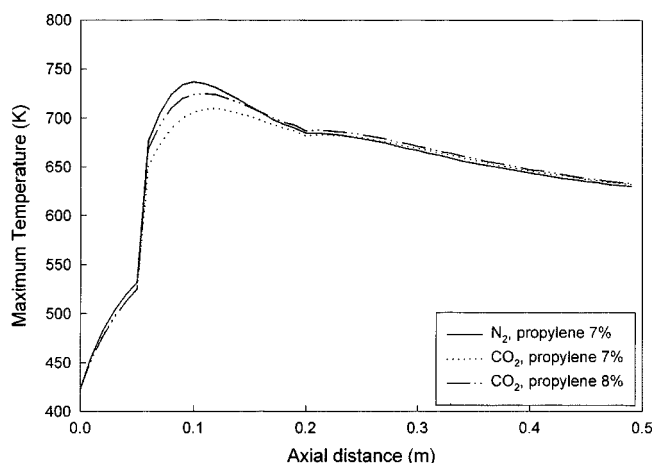
Fig. 5. Calculated maximum temperature of the solid phase along axial distance for experimental conditions shown in Table 1.

Fig. 7. Heat capacity of N_2 and CO_2.

location of maximum temperature in Fig. 4 indicates the hot spot of solid catalyst. When these figures are compared with Fig. 2, it can be shown that the dominant transport resistance falls on the mass diffusion in the catalyst pellets and on the heat transfer between the fluid phase and external catalyst surface. Since the maximum temperature in the solid phase is a major concern from the viewpoint of catalyst lifetime, its profiles also need to be examined. The utilization of CO_2 as a diluent gas instead of N_2 is found to be successful in diminishing the maximum solid phase temperature, as shown in Fig. 5.

The following aspects can explain the role of CO_2 in decreasing the temperature of both fluid and solid phases: thermodynamic and kinematic perspectives. The thermodynamic properties include heat capacity and the kinematic properties encompass viscosity, diffusivity, thermal conductivity, etc. To get an insight into the mechanism of the temperature decrease in the case of CO_2, the effect on temperature of all the differing properties of CO_2 from N_2 was examined through a parametric sensitivity study. The variation of viscosity, diffusivity and thermal conductivity had little effect on the temperature profile. The factors which had large influences on tem-
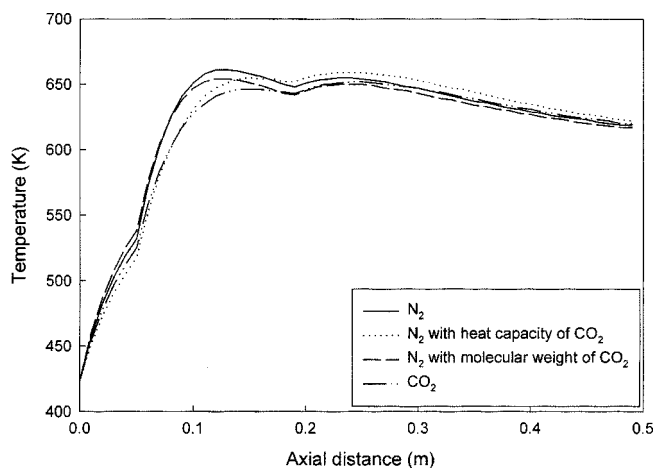
perature were heat capacity and molecular weight (density changed in accordance with molecular weight). Effects of both factors on the fluid phase temperature profile are shown in Fig. 6. Similar trends were observed in solid phase temperature profiles.

The effect of heat capacity can be accounted for easily. Because of its larger heat capacity, CO_2 absorbs more heat than N_2 to reduce the temperature of both fluid and solid phases. The variation of heat capacities with temperature for both diluent gases is shown in Fig. 7.

As for the effect of molecular weight, it is appropriate to find its relationship to kinematic properties to understand the mechanism. The only kinematic parameter that had a relation to molecular weight and had a significant effect on temperature was the wall heat transfer coefficient. Since the wall heat transfer coefficient is generally dependent upon Reynolds number [Calderbank and Pogorski, 1957], it is reasonable to examine what effect molecular weight of CO_2 has on Reynolds number. The Reynolds number and corresponding wall heat transfer coefficient changes due to the adoption of molecular weight of CO_2 are shown in Figs. 8 and 9. Therefore, kinematic viscosity is an important parameter, which can be used to predict temperature change, since Reynolds number is entirely affected by kinematic viscosity under certain operating conditions. Although other properties such as thermal conductivity and Prandtl number

Fig. 6. Calculated axial temperature profile of fluid phase in the case of N_2, N_2 with heat capacity of CO_2, N_2 with molecular weight of CO_2, and CO_2.
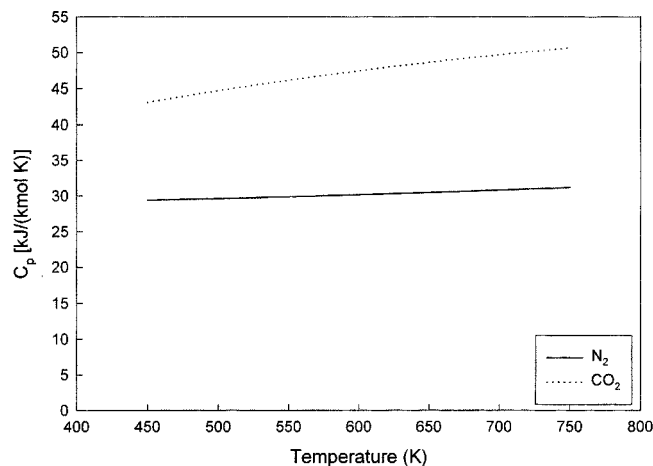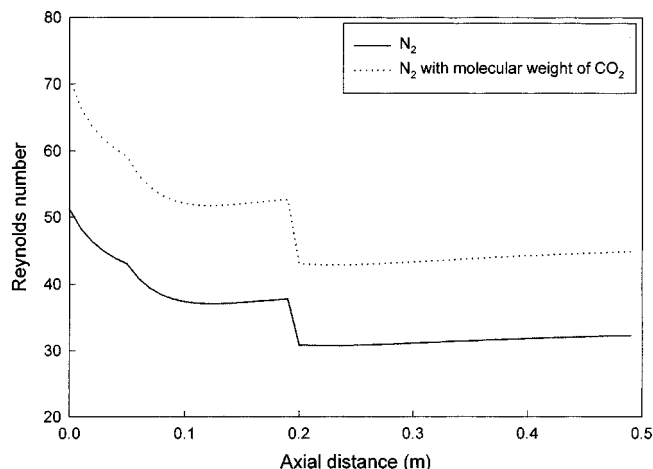

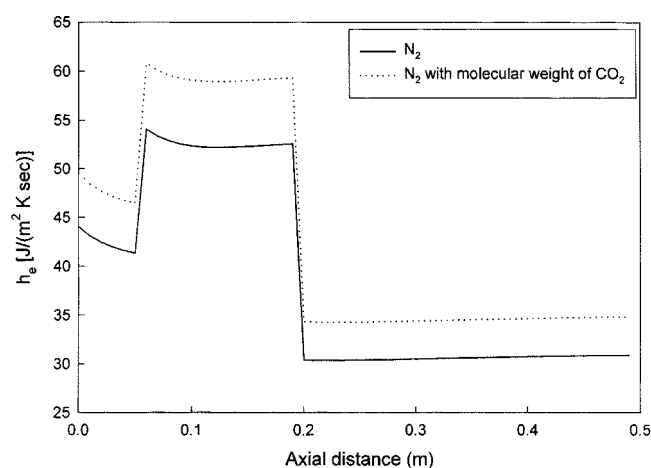**Fig. 8. Effect of molecular weight on Reynolds number in the case of N_2 and CO_2.**

Fig. 9. Effect of molecular weight on heat transfer coefficient in the case of N₂ and CO₂.

also affect heat transfer coefficient, they vary insignificantly.

It has been shown that the temperature of both fluid and solid phases can be lowered via increased heat transport and heat capacity by using CO_2 instead of N_2 as a diluent gas. From the above result, it can be expected that the productivity can be increased through increasing inlet propylene concentration without exceeding the safe operation range if CO_2 is used as a diluent gas. The calculated temperature profiles of fluid and solid phase are shown in Figs. 2 and 5 where inlet propylene concentration is 8 vol% with CO_2 as a diluent gas. The results show that the maximum temperature of the fluid phase is within that of the standard case; therefore, it will be considered as a safe operating condition, since the maximum temperature of fluid phase is a measure of safety. Fig. 5 clearly shows that catalyst lifetime will not be affected by increasing inlet propylene concentration to 8 vol% with CO_2 as a diluent gas. Fig. 2 shows that the modeling result is in good agreement with the experimental result. Although it was in the safe operation range, the propylene conversion was slightly lower in the case of 8 vol% propylene concentration with CO_2 as a diluent gas than that of 7 vol% propylene concentration with N_2 as a diluent gas. The lower conversion is due to a decrease in reaction temperature. To compensate for the decrease in propylene conversion, the inlet coolant temperature increased in the numerical simulation. The results of increasing the inlet coolant temperature are shown in Table 2. The propylene conversion increased and the fluid phase maximum temperature was within the safe operation range. The results show that the utilization of CO_2 as a diluent gas can improve productivity up to 14% within the safe operation condition by increasing inlet propylene concentration from 7 to 8 vol% and coolant temperature.

CONCLUSIONS

A heterogeneous model, which accounts for intraparticle gradients, was used to simulate the partial oxidation reaction of propylene in a single tubular reactor, representing one of many tubes in a multi-tubular reactor. It was made clear that the temperature of the fluid phase and solid phase was lowered when CO_2 was used instead of N_2 as a diluent gas through the calculation with this model. It was proven that large heat capacity and low kinematic viscosity were the main causes of diminishing temperature in the present operating conditions. The other parameters did not show any significant effect on temperature. Thus the results can provide a guideline for selecting an inert gas used in partial oxidation reactions. The model was then applied to the condition in which the inlet propylene concentration was higher than normal operating condition with CO_2 as a diluent gas. The temperature of both fluid and solid phase was sufficiently within the limit, but the propylene conversion was less than that of N_2 as a diluent gas. The problem of low conversion was effectively solved by increasing the inlet coolant temperature. It was revealed that increasing productivity was possible while maintaining safety by using CO_2 as a diluent gas in this model reaction system.

NOMENCLATURE

a_v : external particle surface area per unit reactor volume
C_i : molar concentration of component i in the bulk fluid
C_{i0} : molar concentration of component i at the inlet
C_{is} : molar concentration of component i inside solid
C_{is}^s : molar concentration of component i at solid surface
c_p : heat capacity
D_{ea} : effective diffusivity in axial direction
D_{ei} : effective diffusivity of component i
d_p : particle diameter
d_t : internal tube diameter
h_f : heat transfer coefficient
$-\Delta H$: heat of reaction
k_{gi} : mass transfer coefficient of component i
k_j : rate constant for the reaction j (j=1, 2, 3)
M_w : molecular weight
r : radial coordinate inside solid
R : radius of reactor tube
r_i : rate of reaction of component i
T : temperature in fluid
T_0 : temperature at the inlet
T_r : temperature of surroundings
T_s : temperature inside solid

Table 2. Effect of coolant temperature on C₃H₆ conversion and maximum temperature of fluid and solid phase

Inert gas [Propylene (vol%)]	Inlet coolant temperature (K)	Conversion of propylene	Maximum temperature of solid phase (K)	Maximum temperature of fluid phase (K)
N₂ [7]	581	0.846	737	661
CO₂ [8]	581	0.838	725	655
	586	0.839	725	655
	591	0.855	732	661

T_s^s : temperature at solid surface
U : overall heat transfer coefficient
u_s : superficial velocity
z : axial coordinate

Greek Letters
ε : void fraction of packing
λ_e : effective thermal conductivity
λ_{ea} : effective thermal conductivity in axial direction
θ_x : fraction of oxidized sites
ρ_g : density of fluid
ρ_s : density of solid

REFERENCES

Byun, Y. C. and Lee, W. H., "Process for Manufacturing Catalysts for the Acrolein and Methacrolein Production," KR Patent, 99-21570 (1999).

Calderbank, J. J. and Pogorski, L. A., "Heat Transfer in Packed Beds," *Tras. Int. Chem. Eng. (London)*, **35**, 195 (1957).

Carberry, J. J., "Chemical and Catalytic Reaction Engineering," McGraw-Hill, New York (1976).

Choi, J. and Eigenberger, G., "Dampfeinsparung Durch Peiodische Katalysator-Reaktrivierung Bei Der Styrol-Synthese," *Chem.-Ing.-Tech.*, **61**(8), 641 (1989).

Doraiswamy, L. K. and Sharma, M. M., "Heterogeneous Reactions: Analysis, Examples, and Reactor Design," Wiley, New York (1984).

Franzen, E. P., Maycock, R. L., Nelson, L. E. and Smith, W. C., "Tubular Catalytic Reactor with Cooler," US Patent 3147084 (1964).

Froment, G. F. and Bischoff, K. B., "Chemical Reactor Analysis and Design," Wiley, New York (1979).

Jung, K. Y., So, J. H., Park, S. B. and Yang, S. M., "Hydrogen Separation from the H_2/N_2 Mixture by Using a Single and Multi-Stage Inorganic Membrane," *Korean J. Chem. Eng.*, **16**, 193 (1999).

Ko, D., Lee, W. H. and Paek, K. H., "The Preparation Method for Partial Oxidation Catalyst," KR Patent, 177326 (1998).

Petrovic, L. J. and Thodos, G., "Mass Transfer in the Flow of Gases Through Packed Beds," *Ind. Eng. Chem.*, *Fundamentals*, **7**, 274 (1968).

Roach, P. J., "Computational Fluid Dynamics," Hermosa, Albuquerque, N. M. (1972).

Rowe, P. N., Claxton, K. T. and Lewis, J. B., "Heat and Mass Transfer from a Single Sphere in an Extensive Flowing Fluid," *Trans. Inst. Chem. Eng.*, **43**, T14 (1965).

Satterfield, C. N., "Mass Transfer in Heterogeneous Catalysis," *The Massachusetts Institute of Technology*, 78 (1970).

Song, K. H. and Park, K. H., "Process Development of Acrylates," LG Chem research report (1998).

Szekely, J., Evans, J. W. and Sohn, H. Y., "Gas-Solid Reactions," Academic Press, New York (1976).

Tan, H. S., Downie, J. and Bacon, D. W., "The Reaction Network for the Oxidation of Propylene over a Bismuth Molybdate Catalyst," *Can. J. Chem. Eng.*, **67**, 412 (1989).